RADIO OBSERVATIONS OF ASTEROIDS: RESULTS AND PROSPECTS

JOHN R. DICKEL
University of Illinois

Radio observations of the asteroids can provide information on the thermal and dielectric properties of the surface materials and because the radio emission arises somewhat below the surface, the data give some indication of layering. Observational difficulty has limited the investigations to only 6 asteroids; 1 Ceres and 324 Bamberga appear to have a layer of dust covering a more compacted material; the data on 4 Vesta cannot be matched by any current models for the surface; and the results for 18 Melpomene, 31 Euphrosyne and 433 Eros are too incomplete for firm conclusions. Future possibilities include more accurate radiometry of a few selected asteroids of different taxonomic classes and actual resolution of some of the larger objects by aperture synthesis techniques.

Radio observations of small planetary bodies provide unique information on physical parameters of the material in their subsurface layers. The radio emission is of thermal origin and arises on the order of several wavelengths below the surface. Thus the observed brightness depends upon the inward conduction of the heat from the sun and the outward transfer of the radiation. These processes depend upon the properties of the material, particularly its compaction and so a comparison of the data with the brightness of model asteroids can give a measure of the properties.

Because radio data are difficult to obtain and give only a single integrated flux density, they are clearly complementary to those obtained at optical and

infrared wavelengths. The observational information necessary for a full interpretation of the radio results is discussed in Sec. 7, the development of models for comparison with the data is described in Sec. II and the results to date are given in Sec. III. Finally, some future prospects using new techniques are presented in Sec. IV.

I. REQUIRED INFORMATION

Radio Data

Because the asteroids are small, none have yet been resolved with a radio telescope and we can measure only their integrated flux densities. In order to study the heat transfer, we need the temperatures. The flux density and temperature are related through the Planck law and the solid angle of the object:

$$S_\nu = \frac{2h\nu^3}{C^2} \frac{1}{e^{h\nu/kT}-1} \Omega \qquad (1)$$

where S_ν is the flux density at a given frequency ν. The flux density is usually given in units of Jansky (Jy) where 1 Jansky = 10^{-26} Wm^{-2} Hz^{-1}. h is Planck's constant, c is the speed of light, T the temperature, and Ω the solid angle subtended by the object. Thus we need the diameter of the asteroid to actually obtain a temperature. A knowledge of possible multiplicity is also important in evaluating the size.

Because the asteroids are typically black bodies at temperatures near 200 K, their spectra are peaked in the infrared, and the radio intensities are very low. This fact, coupled with the small diameters, makes their detection difficult. The observations require many hours of integration with the world's largest radio telescopes and careful subtraction of the sky background.

The data presented in Table I were obtained in December 1978 with the 100-meter telescope of the Max Planck Institute for Radioastronomy in Bonn. I observed at a wavelength of 2 cm using a cooled radiometer which was continually switched between two beams separated by 3 arcmin in the sky. The procedure was to scan across the source in the direction of the beam separation so that the difference signal between the two beams produced first a negative response and then a positive response, with the characteristic beam pattern. A total of about 30 observations of 50 scans each were made per asteroid. This required about 20 hours of telescope time each, including some period for calibration. The primary calibration standard was 3C48 for which a flux density of 2.0 Jy at the 2-cm wavelength was adopted. Atmospheric extinction was monitored by regular observations of secondary calibration sources very near the asteroids in the sky.

A final requirement for the radio observations is accurate ephemerides. The telescopes typically have half-power beamwidths of about 1-arcmin and

TABLE I

Radio Observations of Asteroids

Object	T_B	λ	Phase Angle	Dist. from Sun (AU)	Type	Assumed Diam. (km)	Remarks	Ref.
1 Ceres	<150>	3 mm-3.7 cm	8°	2.6	*C*	980	dust on rock	1,2,3
4 Vesta	210±27	3 mm	<~5°	2.4	*U*	500	no good fitting models	3
18 Melpomene	<300	2 cm	~20°	2.1	*S*	152	--	5
31 Euphrosyne	151±30	2 cm	~18°	2.4	*CM*	333?	need IR data	5
324 Bamberga	188±50	2 cm	-23°	2.0	*C*	251	probably thin compacted dust	5
433 Eros	<460	2 cm	<~5°	1.1	*S*	12x24	--	4

References:

1. Andrew (1974).
2. Briggs (1973).
3. Conklin *et al.* (1977).
4. Pauliny-Toth *et al.* (1976).
5. This chapter.

so we must track the asteroids to within a few arcsec. Because we cannot see them directly but must integrate blindly for several hours, the predicted positions must be precise.

Other Data on the Asteroids

The models for the study of heat transfer depend upon the insolation which varies with time because of asteroid rotation. We thus need the rotation period and orientation of the pole, based generally upon optical photometry.

The thermal budget also depends on the amount of energy available, or the albedo of the object. This requires good optical polarimetry and/or optical plus infrared photometry. Finally infrared and radio flux densities – preferably as a function of phase angle or at least at the same phase angle – are important to determine the emissivity of the material. Much of the support information can be obtained from the TRIAD file (see Part VII of this book).

Properties of Materials

In the following model analysis we shall relate the heat transfer to a parameter called the thermal inertia which is given by $(k\rho s)^{1/2}$ where k is the thermal conductivity in cal cm^{-1} sec^{-1} K^{-1}, ρ is the density in cm^{-3}, and s is the specific heat of the material in cal gm^{-1} K^{-1}. The values of these parameters are quite uncertain for many materials. We generally use values within the ranges given by Fountain and West (1970), Robie and Hemingway (1971), Cremers (1972), Cremers and Hsia (1973) and Hemingway, *et al.* (1973) for typical terrestrial and lunar basalts in solid and loose states of compaction. To investigate the transfer of the emergent radiation the dielectric constant ϵ and the electrical loss tangent tan Δ must be set to appropriate values for each material (Campbell and Ulrichs 1969; Bassett and Shackleford 1972). If ice is important, the properties of this material can be taken from Evans (1965).

II. THE MODELS

Structure

The general approach in modeling the radio emission from an asteroid is to adopt a two layer surface for the object: a base region of rock or other dense substance, with an overlying layer of less compacted material. The thickness of the top layer can be varied as well as the thermal and electrical properties of each region. Sample properties for a model of Ceres to match observations by Conklin *et al.* (1977) are listed in Table II.

TABLE II

Parameters for Ceres

OBSERVED		
Radius	490 km	
Albedo	0.04	
Rotation Period	9 hr	
Heliocentric Distance	2.72 AU (Dec 1975)	
Geocentric Distance	1.77 AU (dec 1975)	
Phase Angle	8°.2 (Dec 1975)	
Observing Wavelength	3.33 mm	
Observed Flux Density	0.374×10^{-23} erg sec^{-1} cm^{-2} Hz^{-1}	
MODEL	**UPPER LAYER**	**LOWER LAYER**
Composition	dust	basalt
Thickness	0.5 cm	– –
Absorption Length	2.1 cm	0.36 cm
Dielectric Constant	2.9	7.2
Loss Tangent	0.015	0.054
Density	1.0 g cm^{-3}	2.6 g cm^{-3}
Specific Heat	0.09 cal g^{-1} K^{-1}	0.10 cal g^{-1} K^{-1}
Thermal Conductivity	2×10^{-6} cal cm^{-1} sec^{-1} K^{-1}	4×10^{-3} cal cm^{-1} sec^{-1} K^{-1}
IR Emissivity	0.99	
Scale Depth	2.9 cm	
PREDICTED BRIGHTNESS TEMP.	142 K	

Temperature

The procedure for analysis is to integrate the equation of conductive transport of the heat from the incoming solar radiation downward into the planet. For the numerical integration, the planet can be typically divided into zones 30° in latitude by 30° in longitude over which the temperature and insolation are averaged. If the time step in the integrations is set equal to 1/400 rotation and 8 full rotations of the planet are completed before the final temperatures are read, the averaging procedures are found to be accurate to within 2 %. The step size in depth should be a small fraction of the thermal wavelength given by $L_t = (Pk/\rho s\pi)^{1/2}$ where P is the rotation period and the other symbols are as defined above. Figure 1 shows sample profiles of the temperature distribution with depth at various phase angles for the parameters given in Table II for a model of Ceres. At a given spot, the input of heat necessary to raise the temperature a certain amount is given by $(\rho s/k)^{1/2}$ but the conductivity also enters to carry the heat away so that the final temperature is governed by the thermal inertia $(k\rho s)^{1/2}$. This quantity thus measures the effective resistance of the medium to heating. Note that the low thermal inertia in the upper layer causes large variations in the surface

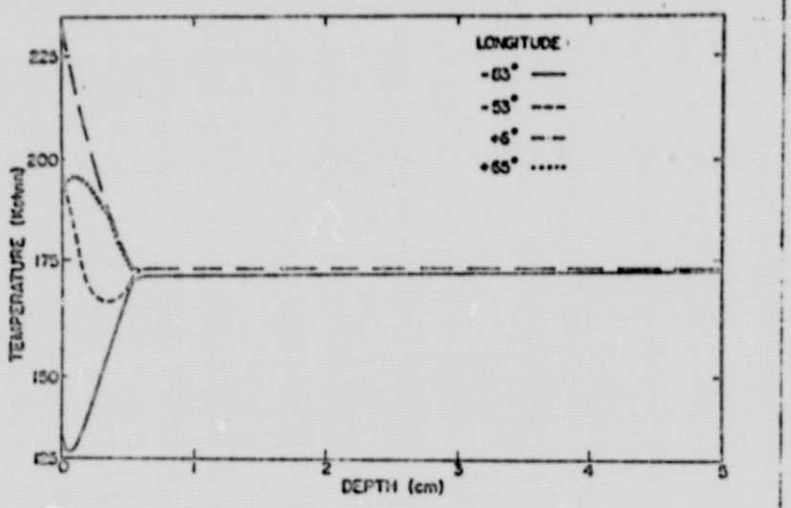

Fig. 1. Profiles of the temperature distribution with depth into Ceres for several phase angles using the model parameters given in Table II.

temperature with phase angle and a steeep gradient with depth but then the thermal wave literally hits a stone wall at the interface between the layers. In the rock, the greatly increased thermal inertia allows a much deeper thermal wave but of much lower amplitude. The rapid spin of the asteroids never allows the thermal wave to penetrate very deeply into the body. Further, these bodies have sufficiently low mean temperatures so that possible radiative transfer of energy (e.g., Linsky 1966) will be negligible and only conduction need be considered.

Radiation

Next the equation of radiative transfer must be integrated outward through the medium taking into account reflections at the interfaces of the different media. The dielectric constant ϵ affects the reflection and emissivity at each interface. In addition, within each zone there is a phase change in the wave as it propagates, which makes self-interference or an effective absorption. This is dependent upon the loss tangent, $\tan \Delta = 2\sigma\lambda/c\epsilon$ where σ is the electrical conductivity, λ the wavelength, and c is the speed of light. With these values of the absorptivity and emissivity for each depth at its given temperature, plus the reflectivities we can determine the emergent intensity at each point on the planet. Finally, the intensity is integrated over the visible disk to give the expected brightness temperature at the phase angle of interest.

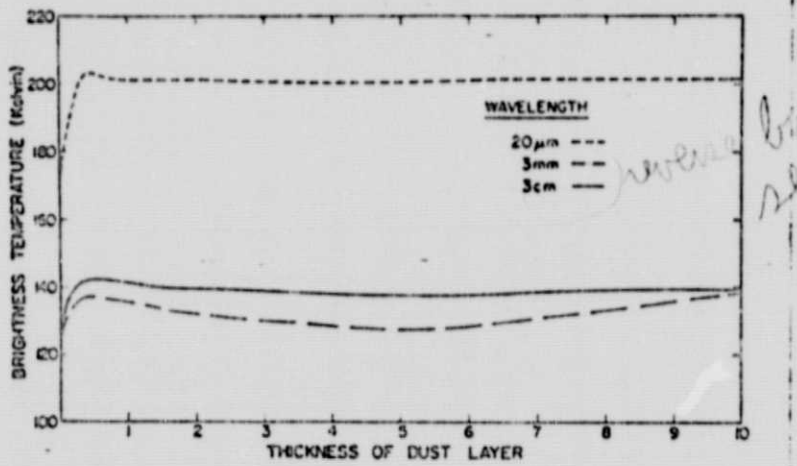

Fig. 2. The brightness temperature of Ceres at a phase angle of 0° as a function of the thickness of the surface dust layer at 3 different wavelengths.

Discussion

To see the effect of some of the parameters, let us look at Fig. 2 which is a plot of the apparent brightness temperatures at different wavelengths for a phase angle of 0° as a function of the depth of the top dust layer. We first note that the infrared temperature is much higher than the radio ones, and this is expected since the infrared emission arises much closer to the surface where the thermal wave has its greatest amplitude. The infrared temperature would, of course, be much lower than the radio ones when the sun is not illuminating the surface near phase angles of 180°. A large difference in temperature is found between models with pure rock and those with a dust cover, even at the long wavelengths which arise in deep layers where little thermal variation is experienced. This is because a pure rock surface with its higher heat capacity and also greater conductivity never has a chance to heat up as much as does one with even a thin dust cover, so that a planet without dust has a lower mean temperature throughout.

In a dusty zone, the dielectric constant is low, producing lower reflectivity and higher emissivity and thus a higher apparent brightness temperature. Although tan Δ is proportional to $1/\epsilon$, the dust has a much lower electrical conductivity and thus a lower loss tangent. The net result is that the penetration depth of the radio wave, $L_R = 2\pi \epsilon^{1/2} \tan \Delta)^{-1}$ is large. The emergent wave will arise deep down but the low thermal inertia limits the thermal wave to a very shallow depth. In rock, the parameters go the opposite way, however, and with a dust layer of about 0.5-1 cm thickness on top of

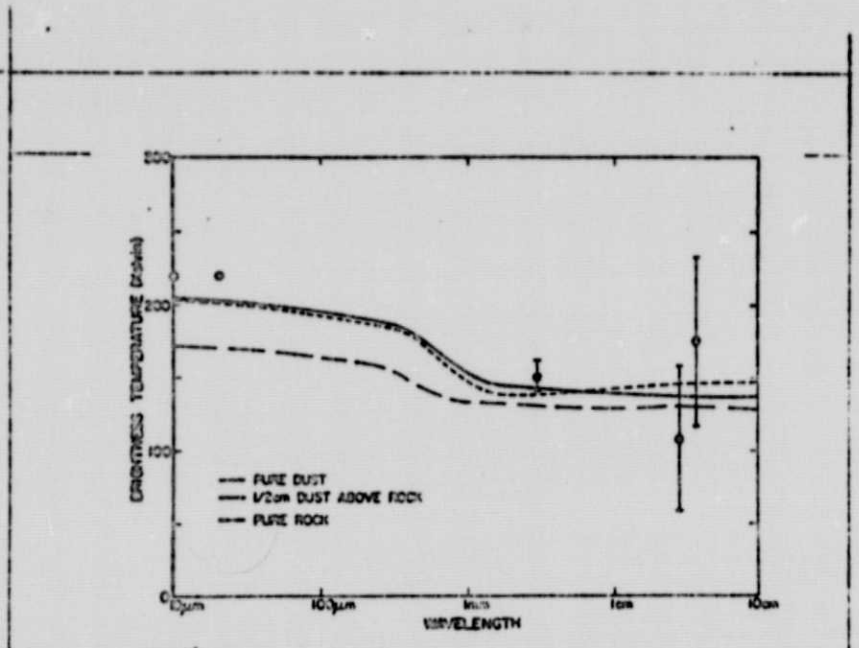

Fig. 3. Brightness temperature spectrum of 1 Ceres. The observed values represented by the points are from: 10 μm and 20 μm – Cruikshank and Morrison (1973); 3 mm – Conklin *et al.* (1977); 2.8 cm – Andrew (1974); 3.4 cm – Briggs (1973). The models represented by the lines are for various thicknesses of dust overlying rock as described in the text.

rock, we find that the net thermal and radio depths in the mixed medium are about equal ($L_R/L_T\lambda \sim 1$). This configuration produces a maximum value in the observed brightness temperature. With more dust, the thermal wave is damped before reaching the depth where radio emission occurs – with less dust, the thermal wave is so deep that it has very small amplitude.

III. RESULTS

Because of the observational problems discussed above, the result of radio observations to date are not many. They are all presented in Table I. Ceres is the only object for which more than one radio measurement exists and its other parameters are quite reliably determined. The comparison of the observational data with various models of this asteroid is illustrated in Fig. 3 (Conklin *et al.* 1977). Although variations of the thermal and dielectric properties of a given layer by as much as a factor of two generally affect the results by less than the uncertainties in the observations, we can draw some conclusions. Clearly pure rock cannot reproduce the observed values, but it is not possible to establish the thickness of the dust layer. As can be seen from Fig. 3, only a very accurate measurement at a wavelength of 10 cm or longer can provide some discrimination of the depth of the dust. Furthermore, the difference between rock and very compacted regolith cannot be distinguished.

The data for the other asteroids in Table I are less complete and so the conclusions in the remarks column can be considered only qualitative. Vesta is certainly unusual, however. Its relatively high radio brightness temperature is about the same as the infrared temperature and no reasonable surface materials have been found to model this behavior (Conklin *et al.* 1977).

IV. PROSPECTS

We can see that microwave radiometry is a viable technique to give clues on the structure of the surface layers of the asteroids, but it is only practical for a few specific objects for which we have good geometrical, optical and infrared data. It can be used to look at representative examples of the various taxonomic classes to see if the different exterior characteristics show differences in their near-subsurface properties. To this end it is important that we get an actual measurement of an *S*-type object.

Another possible contribution of radio observations in the future would be the resolution of some of the larger asteroids for possible satellites and binary pairs. The Very Large Array of radio telescopes has an angular resolution of about 0.1 arcsec at a wavelength of 1.3 cm and should be able to detect any asteroid with a diameter greater than about 0.2 arcsec. Thus any pair of objects satisfying the following conditions should be measurable:

1) resolution: $\left[\frac{\text{separation (in km)}}{\text{distance from earth (in AU)}}\right] > 200$

2) sensitivity: $\left[\frac{\text{diameter (in km)}}{\text{distance from earth (in AU)}}\right]^2 > 25{,}000$

3) preferably an orbital period of the satellite of several days.

Acknowledgments. I gratefully acknowledge the help of W. Altenhof and R. Marcum in making the 2-cm observations a success. B. Marsden provided ephemerides and P. Stumpf helped with both ephemerides and general problems with the computer of the Max Planck Institute. D. T. Ther participated actively in the model analysis. Financial assistance was provided by a grant from the National Aeronautics and Space Administration and by the Netherlands-America Commission for Eductional Exchange through the Fulbright-Hays program during my sabbatical leave at the Leiden Observatory.

REFERENCES

Andrew, B. H. 1974. Radio observations of some minor and major planets. *Icarus* 22: 454-458.

Bassett, H. L., and Shackleford, R. G. 1972. Dielectric properties of Apollo 14 lunar

samples at microwave and millimeter wavelengths. *Proc. Third Lunar Sci. Conf.* Vol. 3, ed. D. R. Criswell (Cambridge: Massachusetts Inst. Technology Press), pp. 3157-3160.

Briggs, F. H. 1973. Radio emission from Ceres. *Astrophys. J.*, 184: 637-639.

Campbell, M. J. and Ulrichs, J. 1969. Electrical properties of rocks and their significance for lunar radar observations. *J. Geophys. Res.* 74: 5867-5881.

Conklin, E. K.; Ulich, B. L.; Dickel, J. R.; and Ther, D. T. 1977. Microwave brightnesses of 1 Ceres and 4 Vesta. In *Comets, Asteroids, and Meteorites*, ed. A. Delsemme (Toledo, Ohio: University of Toledo Press), pp. 257-260.

Cremers, C. J. 1972. Thermal conductivity of Apollo 14 fines. *Proc. Third Lunar Sci. Conf.*, Vol. 3, ed. D. R. Criswell (Cambridge: Massachusetts Inst. Technology), pp. 2611-2617.

Cremers, C. J., and Hsia, H. S. 1973. Thermal conductivity and diffusivity of Apollo 15 fines at low density. *Proc. Fourth Lunar Sci. Conf.*, Vol. 3, ed. W. A. Gose (New York: Pergamon Press), pp. 2459-2464.

Cruikshank, D. P., and Morrison, D. D. 1973. Radii and albedos of asteroids 1, 2, 3, 4, 6, 15, 51, 433, and 511. *Icarus* 20: 477-481.

Evans, S. 1965. Dielectric properties of ice and snow. A review. *J. Glaciology*, 5, 773-792.

Fountain, J. A., and West, E. A. 1970. Thermal conductivity of particulate basalt as a function of density in simulated lunar and martial environments. *J. Geophys. Res.* 75: 4063-4069.

Hemingway, B. S.; Robie, R. A.; and Wilson, W. H. 1973. Specific heats of lunar soils, basalt, and breccia from the Apollo 14, 15 and 16 landing sites, between 90 and 350° K. *Proc. Fourth Lunar Sci. Conf.*, Vol. 3, ed. W. A. Gose (New York: Pergamon Press), pp. 2481-2487.

Linsky, J. L. 1966. Models of the lunar surface including temperature-dependent thermal properties. *Icarus* 5: 606-634.

Pauliny-Toth, I. I. K.; Witzel, A.; and Dickel, J. R. 1976. Upper limit to the 2-cm brightness temperature of asteroid 433 Eros. *Icarus* 28: 147.

Robie, R. A., and Hemingway, B. S. 1971. Specific heats of the lunar breccia (10021) and olivine dolerite (12018) between 90° and 350° Kelvin. *Proc. Second Lunar Sci. Conf.*, Vol. 3, ed. A. A. Levinson (Cambridge: Massachusetts Inst. Technology), pp. 2361-2365.